



HAL
open science

Immobilization of a molecular Re complex on MOF-derived hierarchical porous carbon for CO₂ electroreduction in water/ionic liquid electrolyte

Domenico Grammatico, Huan Ngoc Tran, Yun Li, Silvia Pugliese, Laurent Billon, Bao-Lian Su, Marc Fontecave

► To cite this version:

Domenico Grammatico, Huan Ngoc Tran, Yun Li, Silvia Pugliese, Laurent Billon, et al.. Immobilization of a molecular Re complex on MOF-derived hierarchical porous carbon for CO₂ electroreduction in water/ionic liquid electrolyte. *ChemSusChem*, 2020, 13 (23), pp.6418-6425. 10.1002/cssc.202002014 . hal-02950396

HAL Id: hal-02950396

<https://univ-pau.hal.science/hal-02950396>

Submitted on 13 Dec 2022

HAL is a multi-disciplinary open access archive for the deposit and dissemination of scientific research documents, whether they are published or not. The documents may come from teaching and research institutions in France or abroad, or from public or private research centers.

L'archive ouverte pluridisciplinaire **HAL**, est destinée au dépôt et à la diffusion de documents scientifiques de niveau recherche, publiés ou non, émanant des établissements d'enseignement et de recherche français ou étrangers, des laboratoires publics ou privés.

1 **Immobilization of a molecular Re complex on**
2 **MOF-derived hierarchical porous carbon for**
3 **CO₂ electroreduction in water/ionic liquid**
4 **electrolyte**

5
6
7 *Domenico Grammatico,^{1,3} Huan Ngoc Tran,² Yun Li,² Silvia Pugliese,^{1,2} Laurent Billon,³*

8 *Bao-Lian Su^{1*} and Marc Fontecave^{2*}*

9
10 ¹ Laboratory of Inorganic Materials Chemistry (CMI), University of Namur, 61 rue de
11 Bruxelles, B- 5000 Namur, Belgium.

12
13
14 ² Laboratoire de Chimie des Processus Biologiques, UMR CNRS 8229, Collège de France-
15 CNRS-Sorbonne Université, PSL Research University, 11 Place Marcelin Berthelot, 75005
16 Paris, France.

17
18 ³ Bio-inspired Materials Group: Functionality & Self-assembly, Université de Pau et des Pays
19 de l'Adour, E2S UPPA, CNRS, IPREM UMR 5254, 64000, PAU, France

20
21 * to whom correspondence should be addressed : marc.fontecave@college-de-france.fr;
22 bao-lian.su@unamur.be

23
24 **KEYWORDS:** CO₂ electroreduction; catalysis; rhenium complex; heterogenization;
25 hierarchical porous carbon

26

27 **Abstract**

28 The development of molecular catalysts for CO₂ electroreduction within electrolyzers requests
29 their immobilization on the electrodes. While a variety of methods have been explored for the
30 heterogenization of homogeneous complexes, we here report a novel approach using a
31 hierarchical porous carbon HPC material, derived from a Metal Organic Framework, as a
32 support for the well-known molecular catalyst [Re(bpy)(CO)₃Cl] (bpy = 2,2'-bipyridine). This
33 cathodic hybrid material, named HPC@Re, has been tested for CO₂ electroreduction using a
34 mixture of an ionic liquid (1-Ethyl-3-methylimidazolium tetrafluoroborate EMIM) and water
35 as the electrolyte. The present study reveals that HPC@Re is a remarkable catalyst, enjoying
36 excellent activity (high current densities and high turnover numbers) and good stability.
37 Interestingly, it catalyzes the conversion of CO₂ into a mixture of carbon monoxide and formic
38 acid, with a selectivity that depends on the applied potential. These results emphasize the
39 advantages of integrating molecular catalysts onto such porous carbon materials for developing
40 novel, stable and efficient, catalysts for CO₂ reduction.

41 Introduction

42 Carbon dioxide electroreduction into energy-dense carbon-based liquid or gaseous products is
43 an attractive way to store renewable energies into chemical energy. However, because of the
44 high stability of CO₂ and the requirement of multiple electron and proton-transfers for its
45 transformation, catalysts are required to overcome the slow kinetics, minimize overpotentials
46 and control product selectivity. While heterogeneous catalysts are generally favored due to their
47 stability as well as facile product and catalyst recovery, homogeneous molecular metal
48 complexes (coordination and organometallic complexes) have also been developed since the
49 1980's. In particular, they offer the unique opportunity to tune the coordination environment of
50 the metal center and its reactivity *via* synthetic modifications of the ligands. The molecular
51 strategy has been recently described in review articles.^[1,2]

52 To reconcile these two approaches, homogeneous catalysts have sometimes been immobilized
53 on heterogeneous conductive supports. However, this strategy has been applied to few
54 molecular catalysts with limited success so far.^[3-5] To illustrate the various techniques
55 developed for providing access to modified electrodes, the case of the prototypical catalyst
56 [Re(bpy)(CO)₃Cl] (bpy = 2,2'-bipyridine), highly selective for CO₂ to CO conversion, is
57 interesting, since its immobilization has been studied using a variety of approaches. The first
58 attempts to immobilize such complexes were achieved by Meyer and coworkers^[6] and Abruña
59 and coworkers^[7] in 1985 and 1986, respectively, two years after the initial publication by Lehn
60 reporting the catalytic activity of this complex for CO₂ reduction.^[8] In both cases, the catalyst
61 was immobilized *via* electropolymerization of [Re(vbpy)(CO)₃Cl] (vbpy = 4-vinyl-4'-methyl-
62 2,2'-bipyridine) on an electrode to afford catalytic poly-[Re(vpby)(CO)Cl] films, allowing
63 electroreduction of CO₂ to CO with very high faradaic yields in CH₃CN. However, these films
64 were shown to exhibit limited stability. A similar polymerization approach was recently
65 developed by Kubiak and co-workers using 5-ethynyl-bipyridine derivatives, instead of vinyl-
66 bipyridine, however, in that case very fast deactivation of the catalytic films was observed.^[9] A
67 different strategy for electropolymerization of a variant of Re(bpy)(CO)₃Cl was reported by
68 Deronzier and co-workers.^[10] Upon electrochemical oxidation of a solution of
69 Re(pyrbpy)(CO)₃Cl (pyrbpy = 4-(4-Pyrrol-1-ylbutyl)4'-methyl-2,2'-bipyridine) using a Pt
70 electrode, a polypyrrole-based film was deposited and found to catalyze the electroreduction in
71 CH₃CN of CO₂ leading to CO as the only reduction product. However, the polymer was highly
72 unstable and substantial loss of current was observed during electrolysis. In 1993, Kaneko and
73 co-workers reported the immobilization, *via* simple adsorption, of Re(bpy)(CO)₃Br within a

74 Nafion[®] membrane, which is conductive and stable in various solvents and easily interfaces
75 with electrode surfaces.^[11] The polymer-confined catalyst was active for CO₂ electroreduction
76 in neutral aqueous electrolyte, leading to mixtures of CO, H₂ and formic acid, with a selectivity
77 depending on the applied potential.

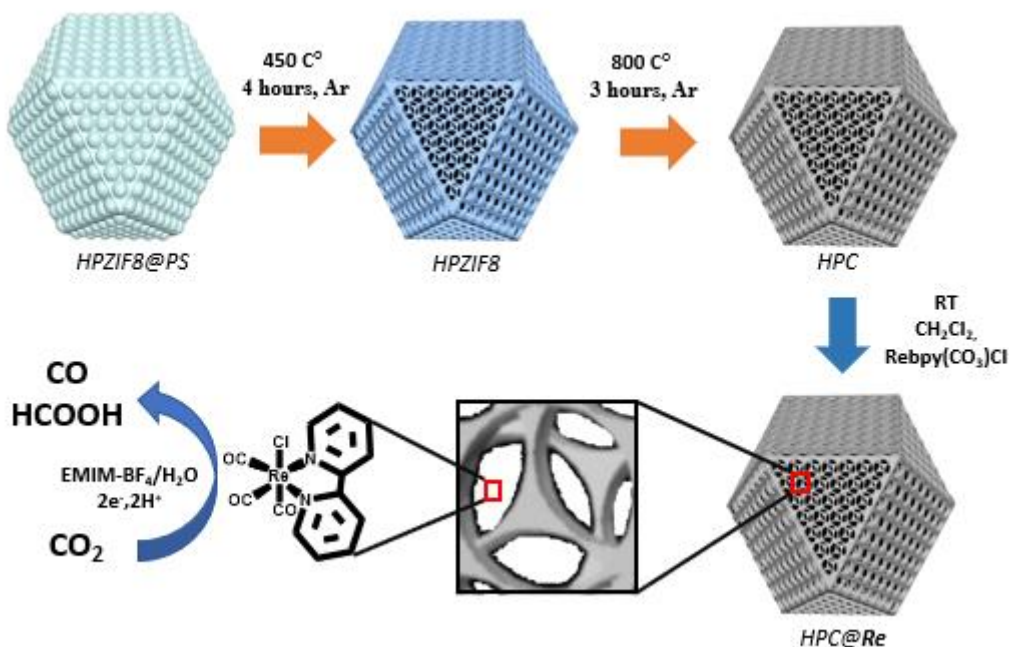
78 Besides this immobilization involving polymers and membranes, covalent grafting to the
79 electrode has also been explored. As *o*-quinone moieties found on the edge planes of graphite
80 can condense with substituted *o*-phenylenediamines, Re(5,6-diamino-phenanthroline)(CO)₃Cl
81 was used to modify graphite electrodes.^[12] The increased conjugation between the catalyst and
82 the electrode was proposed to overcome poor conductivity issues in other polymeric films
83 deposited onto electrodes. This system was very selective for CO formation (faradaic yield of
84 96%) in CH₃CN with high TONs. A conjugated polymer material incorporating
85 Re(bpy)(CO)₃Cl motifs and covalently attached to a glassy carbon electrode was obtained by
86 electropolymerization of a Re complex containing 2,2'-bipyridine-5,5'-bis-(diazonium)
87 ligands.^[13] These molecular films proved highly stable, allowing thousands of turnovers for
88 selective production of CO in CH₃CN.

89 Finally, non-covalent immobilization was achieved, exploiting π - π interactions between
90 pyrolytic graphite and Re(pyrene-bpy)(CO)₃Cl, containing a pyrene-substituted bpy.^[14] This
91 system was catalytically active for CO production but was rapidly deactivated, likely because
92 of reduction of the pyrenyl moiety. The best result with such a non-covalent immobilization
93 strategy was obtained by Kubiak and co-workers who developed a hybrid electrode resulting
94 from the incorporation of Re(tBu-bpy)(CO)₃Cl, with tBu-bpy = 4,4'-di-*tert*-butyl-2,2'-
95 bipyridine, into multi-walled carbon nanotubes (MWCNTs). This material proved stable and
96 active in an aqueous electrolyte for highly selective CO production, at relatively low
97 overpotential and with a current density of 4 mA.cm⁻².^[15]

98 One of the drawbacks of all these immobilization strategies, with the exception of the MWCNT/
99 Re(tBu-bpy)(CO)₃Cl system, resides in the need to introduce functionalities to the bipyridine
100 ligand. This not only generates synthetic issues but also results in significant modifications of
101 the electronic properties of the catalyst as well as of its reactivity. We thus thought of
102 developing methods that allow the immobilization of the [Re(bpy)(CO)₃Cl] itself without
103 synthetic modifications. Here we report the preparation and characterization of an original
104 conductive carbon porous material and its utilization as a support for the [Re(bpy)(CO)₃Cl]
105 catalyst, which can be easily fixed within the pores of the solid material. The novel hybrid
106 material proved stable and active as a catalyst for CO₂ electroreduction, with high current

107 densities and high turnover numbers. Interestingly, this catalyst converts CO₂ into a mixture of
108 CO and HCOOH, whose ratio depends on the applied potential.

109



110

111 **Scheme 1:** Synthesis of HPC and HPC@Re.

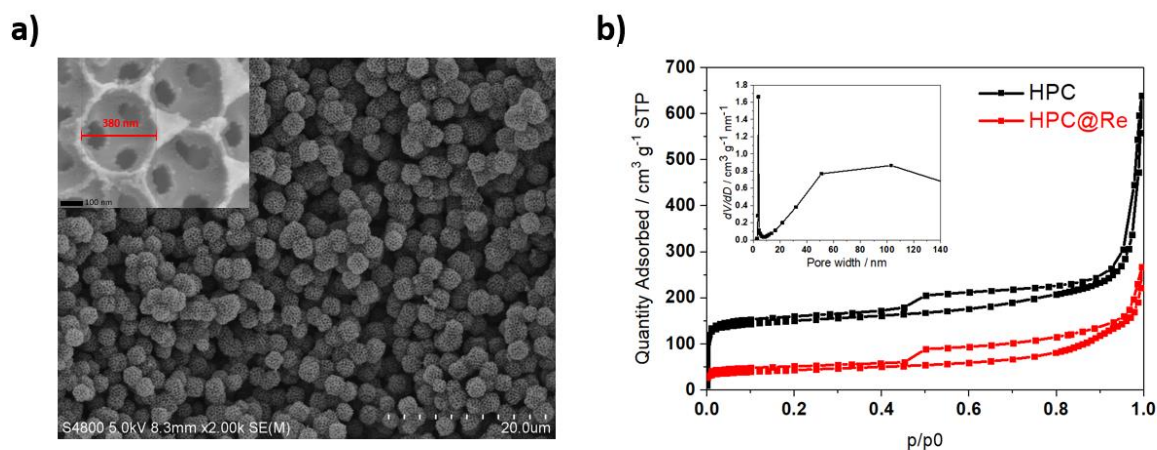
112

113 RESULTS AND DISCUSSION

114 Synthesis and characterization of the hierarchical porous ZIF8-derived carbon-HPC

115 The synthesis of hierarchical porous carbon (named HPC in the following) derived from the
116 Metal Organic Framework ZIF8 was synthesized following a previous report,^[16] however with
117 significant modifications (Scheme 1). First, the ZIF8 precursor was infiltrated into the
118 polystyrene spheres (PS) template and crystallized using a solution of CH₃OH/NH₃·H₂O.
119 Second, a treatment at 450 °C under argon atmosphere, instead of washing with organic
120 solvents used in the previous report,^[16] was carried out in order to remove the PS template and
121 thus obtain the hierarchical porous ZIF8 (HPZIF8). HPZIF8 shows slightly lower BET surface
122 area (Figure S1 and Table S1) as compared to the previous report,^[16] likely due to remaining
123 PS beads in the sample. Scanning electronic microscope (SEM) and powder x-ray diffraction
124 (XRD) characterizations of HPZIF8 show expected well-defined ZIF8 crystals (Figures S2-S3).
125 HPZIF8 was finally pyrolyzed under inert atmosphere at 800 °C to obtain the final hierarchical
126 porous carbon (HPC) material. HPC was characterized by various techniques. XRD pattern

127 confirmed that the material was not crystalline anymore (Figure S2). SEM images (Figure 1a)
 128 showed well-defined and well-distributed carbon particles with a three-dimensional
 129 tetrakaidecahedron morphology and with a uniform (monodisperse) diameter of 2 μm . This
 130 specific morphology is due to the use of PS latex as a template which controls the shape of the
 131 material.^[16] The highly ordered porous carbon material showed a hexagonal-close-packed
 132 arrangement of PS nanospheres ??? (inset Figure 1a) with interconnected windows and porosity
 133 uniformly distributed.^[17,18] N_2 physisorption analyses (Figure 1b and Figure S1) allowed to
 134 establish a BET surface area of $495 \text{ m}^2 \cdot \text{g}^{-1}$ and total pore volume of $1 \text{ cm}^3 \cdot \text{g}^{-1}$ with around 25%
 135 of the total pore volume assigned, by the Horwart-Kawazoe method, to the micropores. The
 136 increase of the surface area due to the pyrolysis step leading to HPC ($495 \text{ m}^2 \cdot \text{g}^{-1}$) from HPZIF8
 137 ($145 \text{ m}^2 \cdot \text{g}^{-1}$) is likely due to a complete removal of PS. N_2 adsorption isotherms are of typical
 138 type I, indicating the microporous character of the material with a pore size located at 0.5 nm.
 139 The presence of mesopores and macropores has been revealed by two N_2 adsorption uptakes at
 140 p/p_0 of 0.5 and 0.95-1.0, respectively, as shown in Figure 1b. The BJH analysis method gives a
 141 very sharp pic centered at 5 nm, corresponding to the hysteresis loop at p/p_0 of 0.5 ^[19] while the
 142 sharp N_2 adsorption uptake at p/p_0 of 0.95-1.0 is generated by the macropores of 380 nm
 143 observed by SEM (Figure 1a). The above analysis suggests HPC material contains a
 144 hierarchical macro-meso-microporous structure.
 145



146
 147 **Figure 1:** a) SEM image of HPC with enlargement (inset); b) N_2 adsorption-desorption
 148 isotherms of HPC and Re@HPC and pore size distribution (inset) made by BJH method of
 149 HPC.

150

151 **Functionalization of HPC material with a molecular complex**

152 HPC was then used as a support for heterogeneizing the molecular $[\text{Re}(\text{bpy})(\text{CO})_3\text{Cl}]$ complex,
153 named Re in the following. Re was immobilized without any further functionalization taking
154 advantage of the interconnected porosity of the support which improves the hosting properties.
155 The heterogenization of Re on HPC has been carried out as follows. First, Re was dissolved in
156 CH_2Cl_2 and the solution added dropwise to a sonicated dispersion of HPC in the same solvent
157 (Scheme 1). The solution was stirred for 1 hour and after centrifugation the supernatant
158 removed. Finally, the as-obtained hybrid system was dried overnight at room temperature. The
159 relative amounts of starting precursors were chosen in order to obtain an initial weight Re:HPC
160 ratio of 1:9. Then, the obtained HPC@Re material was characterized not only to check for the
161 presence of the molecular complex within the solid but also to define morphology and structure
162 of the final material.

163 SEM images of Re@HPC showed that the morphology of the carbon particles was retained
164 (Figure S4). The presence of Re within the solid has been verified by Energy Dispersive X-Ray
165 mapping (EDX) (Figure S4) showing a uniform dispersion of the complex, as well as the
166 presence of residual Zn from ZIF8, even after pyrolysis. N_2 physisorption analysis after Re
167 loading showed a decrease of the BET surface area, indicating clearly the incorporation of the
168 molecular complex within the pores of the support (Figure 1b). The integrity of Re within the
169 solid material was proved by ^1H NMR spectroscopy after releasing the complex from Re@
170 HPC by washing with CDCl_3 . The spectrum of the solution proved identical to that of the pure
171 freshly prepared homogeneous complex (Figure S5). Finally, the amount of extractible complex
172 from 30 mg of HPC@Re using an organic solvent (CH_2Cl_2) was determined by UV-Visible
173 spectroscopy from the intensity of the absorption band at 387 nm, characteristic of the complex
174 (Figure S6). It was determined by ICP-MS that the sample contained $4.8 \mu\text{mol}$ of complex
175 leading to $0,16 \mu\text{mol}/\text{mg}$ of complex within Re@HPC.

176

177 **Preparation and characterization of the working HPC@Re/GDL electrode**

178 An Re@HPC /GDL electrode (1cm^2) was prepared by deposition of 5 mg HPC@Re on a
179 commercial gas diffusion layer (GDL), as described in the experimental section. The total
180 amount of Re in that electrode was determined by UV-Visible spectroscopy as described above
181 for HPC@Re (Figure S6). The electrode was shown to contain $0.6 \mu\text{mol}\cdot\text{cm}^{-2}$. The CV of
182 HPC@Re/GDL electrode in 0.1 M TBAPF₆ in CH_3CN at low scan rate of $10 \text{mV}\cdot\text{s}^{-1}$ (Figure
183 S7) served to calculate the density of electroactive species from the charge integration of the
184 peak at about -1.6V vs Fc/Fc^+ , corresponding to the reoxidation of the complex.^[20] The data

185 led to a high surface density of 20 nmol.cm^{-2} , corresponding to approximately 3% of the total
186 amount of complex present in the solid material. These numbers compare well with those
187 determined for the best hybrid $[\text{Re}(\text{tBu-bpy})(\text{CO})_3\text{Cl}]/\text{MWCNT}$ material (13 nmol.cm^{-2} , 1-8%
188 of the total catalyst loaded) reported by Kubiak *et al.*^[15]

189

190 **Electrocatalytic CO₂RR in water/1-Ethyl-3-methylimidazolium tetrafluoroborate** 191 **(EMIM) electrolyte**

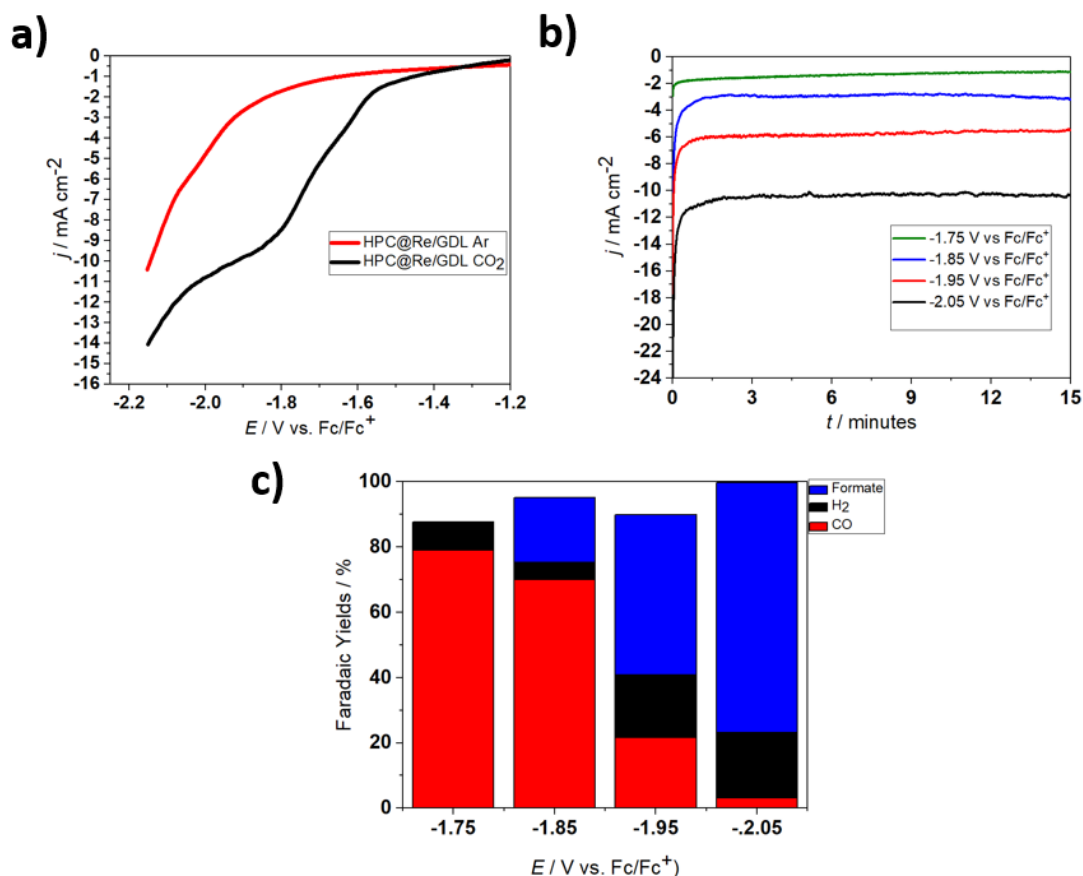
192 Since the electroreduction of CO₂ using the HPC@Re/GDL in water yielded mainly hydrogen
193 (data not shown), the reaction was studied in a CO₂-saturated solution of an ionic liquid in the
194 presence of a small amount of water as a source of protons. Indeed, ionic liquids have been
195 shown to facilitate CO₂ electroreduction catalyzed by solid catalysts due to their ability to
196 increase CO₂ solubility and activate CO₂.^[21] A previous report showed that using an ionic liquid
197 as both the solvent and electrolyte resulted in decreased overpotential and increased second-
198 order rate constant for CO₂ electroreduction to CO catalyzed by $[\text{Re}(\text{bpy})(\text{CO})_3\text{Cl}]$.^[22]
199 However, with such homogeneous systems, the viscosity of the medium results in strong
200 limitations in mass transport (small diffusion coefficients) of the molecular catalyst and low
201 current densities. This issue does not apply to an immobilized molecular complex. Thus, a
202 mixture of an ionic liquid (1-Ethyl-3-methylimidazolium tetrafluoroborate) and water (named
203 H₂O/EMIM in the following) has been chosen as the electrolyte for further CO₂
204 electroreduction studies using the HPC@Re/GDL electrode. The Linear Sweep
205 Voltammograms (LSVs) of the HPC@Re/GDL electrode in 5% v/v H₂O/EMIM saturated with
206 either Ar or CO₂ are presented in Figure 2a. A catalytic wave at an onset potential of -1.55 V
207 vs Fc/Fc⁺ and developing further up to an applied potential of -2.05 V was observed only in the
208 presence of CO₂ and was thus assigned to CO₂ reduction (Figure 2a). At potentials more
209 negative than -2.1 V, a second wave was observed however also present for the HPC@Re/GDL
210 electrode under argon, thus likely corresponding to proton reduction to H₂. Unfortunately, the
211 evaluation of overpotential values is not trivial here as the equilibrium potentials of the
212 CO₂/HCOOH and CO₂/CO couples in H₂O/EMIM are unknown.

213 Controlled Potential Electrolysis (CPE) at different potentials between -1.75 V and -2.05 V
214 versus Fc/Fc⁺ coupled with quantification of CO₂ reduction products has been carried out for
215 15 minutes in order to characterize the CO₂ reduction reaction. As expected the total current
216 density increased with increased driving force up to 11 mA.cm^{-2} at -2.05 V and was found to
217 be stable during electrolysis at all potentials (Figure 2b). The high current densities translate

218 into remarkably high turnover numbers (TONs) and high Turnover Frequencies (TOFs). For
219 example, at -2.05 V, 2026 TONs are reached after 15 min, which corresponds to a TOF value
220 of 2.3 s^{-1} . As shown below, under these conditions, formate was the major product.

221 The only detected products in all experiments were H_2 and CO in the gaseous phase and formic
222 acid in the liquid phase. Surprisingly, the selectivity of the reaction was found to be greatly
223 dependent on the applied potential, with CO being the major product at the most anodic
224 potentials and formic acid becoming the major product at potentials more cathodic than -1.9 V,
225 while H_2 was a minor product at all potentials. This is clearly shown in Figure 2c which displays
226 the Faradaic yields (FY) of the various products at different potentials. At -1.75 V vs Fc/Fc^+ ,
227 $\text{FY}(\text{CO})$ and $\text{FY}(\text{H}_2)$ were 79% (TON_{CO} 258 and TOF_{CO} 0.3 s^{-1}) and 9% respectively, and no
228 formate could be found in the liquid phase. Screening the reaction at more negative potentials,
229 CO formation decreased dramatically while $\text{FY}(\text{HCOOH})$ and $\text{FY}(\text{H}_2)$, the latter to a smaller
230 extent, increased. At -2.05 V, $\text{FY}(\text{CO})$, $\text{FY}(\text{H}_2)$ and $\text{FY}(\text{HCOOH})$ were 3%, 20% and 76%
231 ($\text{TON}_{\text{HCOOH}}$ 1950 and $\text{TOF}_{\text{HCOOH}}$ 2.2 s^{-1}) respectively (Figure 2c). Thus, the selectivity between
232 CO vs HCOOH formation during electroreduction of CO_2 catalyzed by HPC@Re can be finely
233 tuned by varying the applied potential.

234



235

236 **Figure 2:** Controlled potential electrolysis of CO₂ using the HPC@Re/GDL electrode: **a)** LSV
237 in 5% v/v H₂O/EMIM saturated with CO₂ (black) or with Ar (red), scan rate 20 mV.s⁻¹; **b)** total
238 current density at various applied potentials as a function of time; **c)** Faradaic Yields for CO,
239 H₂ and formate after 15 min electrolysis at different potentials in 5% v/v H₂O/EMIM saturated
240 with CO₂.

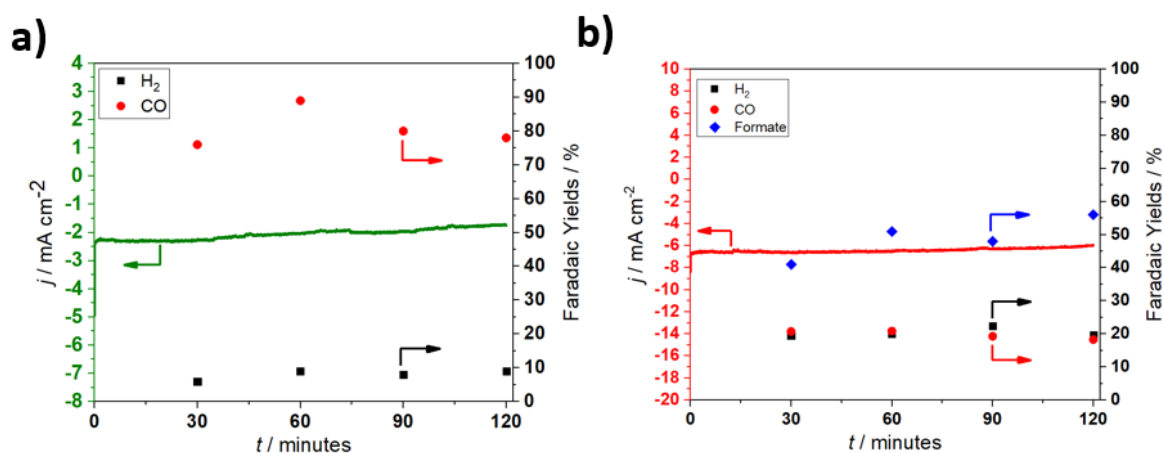
241

242 The observation of formate formation is unexpected since the Re complex is known to be a very
243 selective catalyst for CO₂ electroreduction to CO in organic solvents. Interestingly, when, as a
244 control experiment, CPE was carried out using the soluble Re complex in the same CO₂-
245 saturated 5% v/v H₂O/EMIM electrolyte, the reaction was shown to yield mainly H₂ with minor
246 amounts of CO and almost no HCOOH, at all visited potentials (Figure S8). Furthermore, the
247 current densities were much lower since at -1.85 V the current density reached a value of 0.3
248 mA.cm⁻² (Figure S8) for 12 μmol of Re catalyst (1 mM in 12 ml) as compared to 3 mA.cm⁻²
249 for 0.6 μmol Re catalyst present in HPC@Re/GDL (Figure 2). This thus demonstrates the great
250 impact of the solid support on the reaction outcome, both in terms of the activity and the
251 selectivity. The effect on the activity is likely to be partly due to the hydrophobic nature of the
252 environment provided by the pores in which the catalyst is bound, favouring CO₂ uptake and
253 increasing CO₂ local concentration and to the absence of mass transport limitations which
254 challenge the homogeneous catalyst.

255 In contrast, the effect of the solid support on the selectivity is difficult to explain. Formation of
256 formate cannot be explained by the catalytic properties of the support itself since, as a control
257 experiment, CPE of CO₂ using an HPC/GDL electrode, not loaded with the Re complex, under
258 identical conditions, gave very different results (Figure S9). For example, at -1.85 V, with a
259 current density of 1 mA.cm⁻², no formate could be detected, as compared to 3 mA.cm⁻² and a
260 FY(HCOOH) of 20% for the HPC@Re/GDL electrode, and at -1.95 V, with a current density
261 of 2 mA.cm⁻², a FY(HCOOH) of 15% was obtained, as compared to 6 mA.cm⁻² and a
262 FY(HCOOH) of 50% for the HPC@Re/GDL electrode. There is, to our knowledge, one study
263 reporting formate production during electroreduction of CO₂ catalyzed by the Re complex, with
264 a HCOOH/CO selectivity depending on the applied potential as well.^[11] Interestingly, in that
265 case, the catalyst was incorporated into a Nafion membrane and electrolysis was carried out in
266 a phosphate aqueous electrolyte, explaining why the major product at almost all potentials
267 applied was H₂. The activity, in terms of current density, of that system was furthermore much
268 lower than that reported here. While formate production using the HPC@Re catalyst is likely
269 to proceed *via* a Re-H hydride species reacting with CO₂,^[23,24] in contrast to CO production
270 which derives from a Re-CO₂ intermediate, it is so far unclear why the HPC support favours

271 such a mechanism at very cathodic potentials and how the support tunes the HCOOH/CO
272 selectivity. These mechanistic aspects deserve further investigation.

273 Finally, long-term CPE was carried out for 2 hours at -1.75 V (formation of CO and H₂) and -
274 1.95 V (formation of CO, HCOOH, H₂) vs Fc/Fc⁺ (Figure 3). The system proved very stable
275 during electrolysis in terms of both current density and selectivity. After 2 hours at -1.75 V,
276 3155 TON_{CO} were achieved corresponding to a TOF_{CO} of 0.4 s⁻¹. Furthermore, post-electrolysis
277 characterization of the electrode by SEM showed that the porosity of the system was retained
278 even if slight agglomeration of the particles was observed (Figure S10). Finally, the amount of
279 Re released in solution after 2 hours electrolysis was measured by ICP-MS and found to be
280 within 5 to 10%, from one experiment to another, with respect to the initial amount of Re
281 initially present on the electrode. Based on the results given above (Figure S8), this amount is
282 far too small to account for the CO₂ reduction activity of the electrode.



283
284 **Figure 3:** Long-term electrolysis: current density and FY as a function of time during CPE at -
285 1.75 V vs Fc/Fc⁺ (a) and at -1.95 V vs Fc/Fc⁺ (b) under CO₂ in 5% v/v H₂O/EMIM using the
286 HPC@Re/GDL. Faradaic yields for CO (red dots), H₂ (black squares) and formate (blue
287 diamonds).

288
289
290

291 **Conclusion**

292 We have developed a novel hybrid solid catalyst, HPC@Re, for CO₂ electroreduction to CO
293 and HCOOH. Thanks to the hierarchical porosity of the porous and conductive carbon material
294 HPC, large amounts of the molecular catalyst [Re(bpy)(CO)₃Cl] can be easily immobilized
295 without any functionalization. We anticipate that HPC can be further used for heterogeneization
296 of other complexes. In order to optimize catalysis, CO₂ electroreduction has been studied in an
297 ionic liquid electrolyte in the presence of water, known to favour CO₂ solubility and activation.
298 To the best of our knowledge, this is the first example of a heterogenized molecular complex
299 characterized for CO₂ reduction catalysis in an ionic liquid. HPC@Re/GDL electrodes thus
300 provide high current densities (up to 11 mA.cm⁻²), high TOF_{CO+HCOOH} (2.3 s⁻¹) and display good
301 stability. When compared to other hybrid solid electrodes in which [Re(bpy)(CO)₃Cl] has been
302 immobilized,^[6-15] the HPC@Re/GDL electrode is among the most efficient and stable ones. In
303 addition, this novel electrode is unique in providing not only CO but also HCOOH as CO₂
304 reduction products, with FY(H₂) not exceeding 20%, in marked contrast with the other
305 comparable systems which are selective for CO production and in contrast with the
306 homogeneous catalyst which favours proton reduction over CO₂ reduction and is quite
307 inefficient in the same water/ionic liquid system. The CO/HCOOH ratio can be tuned with the
308 applied potential since it decreased as the potential is shifted to more cathodic values. The
309 combination of a water/ionic liquid electrolyte system, the hierarchical porosity of the support
310 facilitating mass exchange and transfer,^[25] and the hydrophobic environment provided by the
311 pores in which the molecular complex is fixed is likely to explain the remarkable and unique
312 performances of HPC@Re as a CO₂ reduction catalyst. However, further studies are required
313 to understand how the support drives and controls the reactivity of the immobilized complex.

314

315

316

317 **Experimental section**

318 **General methods**

319 All chemicals were received from commercial sources and used as received. Zinc nitrate
320 hexahydrate ($\text{Zn}(\text{NO}_3)_2 \cdot 6\text{H}_2\text{O}$, 99%), 2-methylimidazole (98%), tetrabutylammonium
321 hexafluorophosphate (TBAPF_6 , 98%), Nafion[®] perfluorinated resin (10 μL of a 5 wt% solution
322 in mixture of lower aliphatic alcohols containing 5% water), absolute ethanol ($\text{CH}_3\text{CH}_2\text{OH}$),
323 methanol (CH_3OH , 99%), dichloromethane (CH_2Cl_2 , 99 %), acetonitrile (CH_3CN , 99.8%),
324 chloroform-d (CDCl_3 , 99.8%) and ammonia solution ($\text{NH}_3 \cdot \text{H}_2\text{O}$, 32%) were purchased from
325 Sigma-Aldrich. 1-Ethyl-3-methylimidazolium tetrafluoroborate (>98%) was purchased from
326 IOLITEC Ionic liquid technologies GmbH. $[\text{Re}(\text{bpy})(\text{CO})_3\text{Cl}]$ was synthesized as previously
327 reported by Kubiak *et al.*^[26]

328 UV-vis spectra were recorded using a Cary 100 UV-vis spectrophotometer (Agilent). ¹H
329 spectra were recorded on a Bruker Avance-III 300 NMR spectrometer (300 MHz) at room
330 temperature. The Rhenium concentrations in the electrolyte were assessed using an Agilent
331 7900 quadrupole ICP-MS. Liquid samples were sprayed through a micro-nebulizer in a Scott
332 spray chamber prior to ionization. An indium internal standard was injected after inline mixing
333 with the samples to correct for signal drift. Calibration solutions with Re concentrations
334 encompassing the full range of sample concentrations were used to convert measured counts to
335 concentrations. Reported uncertainties were calculated using algebraic propagation of blank
336 subtraction and sample count standard deviations (n=3).

337 **Material characterization**

338 Scanning electron microscope (SEM) images were performed by using a JEOL 7500F
339 microscope operating at 15kV with EDX detector incorporated and a Hitachi S-4800 operating
340 at 5kV. X-ray diffraction (XRD) characterization was carried out by Panalytical X'Pert PRO
341 diffractometer (Cu $K\alpha$ radiation, Bragg-Brentano geometry, sealed tube operated at 45 mA 30
342 kV X'Celerator linear detector). Nitrogen physisorption analyses were performed with ASAP
343 2420 using a platinum resistance device and liquid nitrogen as adsorbed molecule.

344 **Synthesis of HPZIF8**

345 Polystyrene spheres (PS) (the size of 400 nm) were synthesized as previously reported^[16] and
346 used as a template for the preparation of a hierarchical porous ZIF8 (HPZIF8). HPZIF8 with
347 polystyrene (HPZIF8@PS) was also prepared using a protocol from Chen *et al.*^[16], via
348 infiltration of the ZIF8 precursor into the PS spheres template. The following steps were
349 modified from the previous protocol to obtain the HPZIF8. This, was prepared from

350 HPZIF8@PS treating it at 450 °C during 4 hours under Argon atmosphere for removing the PS
351 beads.

352 **Synthesis of HPC**

353 The hierarchical porous carbon (HPC) derived from ZIF8 was obtained by heating the HPZIF8
354 at 800 °C during 3 hours under Argon atmosphere. The HPC was used without further
355 treatment.

356 **Preparation of HPC@Re**

357 The preparation of Re complex loading on HPC material was carried out as follows: the solution
358 of [Re(bpy)(CO)₃Cl] (6 mg) in CH₂Cl₂ (10 mL) was added dropwise to a sonicated dispersion
359 of HPC (50 mg) in CH₂Cl₂ (20 mL). The suspension was then centrifuged for removing the
360 supernatant. The obtained material was then dried overnight under vacuum condition at room
361 temperature and used without further treatments.

362 These materials were characterized by: N₂ physisorption analyses, SEM images, EDX mapping
363 and XRD (Supporting Information).

364 The amount of Re complex loaded was quantified by UV-Visible spectroscopy (Figure S6):
365 after extraction of 30 mg of HPC@Re with 20 mL of CH₂Cl₂ the solution was analysed for its
366 absorption at 387 nm, characteristic of [Re(bpy)(CO)₃Cl] and the latter was compared to
367 calibration curve prepared with pure [Re(bpy)(CO)₃Cl]. HPC@Re was also treated with CDCl₃
368 for extraction of the complex and characterization by ¹H NMR (Figure S5), in order to confirm
369 the integrity of the complex.

370 **Electrode preparation**

371 HPC@Re (5 mg) was sonicated 1 hour in absolute ethanol (200 μL) and a solution of Nafion
372 perfluorinated resin (10 μL of a 5 wt% solution in mixture of lower aliphatic alcohols containing
373 5% water). The suspension was then, carefully, deposited by drop casting on a gas-diffusion
374 Layer, GDL (AVCarb GDS 3250; 1 cm²) in order to have a uniform deposition. The electrode
375 was then dried in air overnight at room temperature. For all the experiments the working
376 electrodes were prepared in the same way.

377 **Electrode characterization**

378 SEM images of the HPC@Re/GDL electrode were obtained before and after 2 hours
379 electrolysis. The amount of Re complex present on the GDL was quantified by UV-Visible
380 spectroscopy as described above via extraction of the complex from the HPC@Re/GDL
381 electrode immersed in 20 mL of CH₂Cl₂ (Figure S6) and quantification by comparison with the
382 calibration curve.

383 **Electrochemical characterization**

384 All electrochemical characterization and electrolysis experiments were carried out using a Bio-
385 logic SP300 potentiostat with two-compartment cell with an Ag/AgCl/3M KCl reference
386 electrode, placed in the same compartment as the working HPC@Re/GDL electrode. A
387 platinum counter electrode was placed in a separate compartment. The two compartments were
388 separated by a membrane (Fumasep FBM-Bipolar Membrane). The electrolyte was CO₂-
389 saturated 5% v/v H₂O/EMIM (12.5 mL). The electrochemical cell was first purged with CO₂ at
390 a flow rate of 20 mL.min⁻¹ for 1 h prior to catalytic tests using a mass flow controller
391 (Bronkhorst EL-FLOW model F-201CV). All potential values are given versus the potential of
392 the Fc/Fc⁺ couple added as an internal standard to the solution after measurement. In 5% v/v
393 H₂O/EMIM: E_{1/2}(Fc/Fc⁺) = 0.35V vs Ag/AgCl (Figure S11)

394 CVs for the determination of surface density of electrochemically active sites were recorded in
395 CH₃CN, 0.1 M TBAPF₆ with a scan rate of 10 mV.s⁻¹.

396 The surface loading ($\Gamma[\text{Re}]$ as mol.cm⁻²) of the catalyst was calculated through the integration
397 of the reoxidation wave in the CV scan (Figure S7) using the equation:

$$398 \quad \Gamma[\text{Re}] = \frac{q}{nFA}$$

399 where q is the charge (C) obtained from integration of the oxidation wave, n the number of
400 electrons in the redox process per Re center (n = 1), F is the Faraday constant (96485 C.mol⁻¹),
401 and A is the geometrical electrode area (1 cm²).^[27]

402 The homogeneous electrochemical experiments were carried out under the same conditions
403 described above using the same electrochemical cell. A glassy carbon electrode (1 cm²) was
404 used as working electrode in a solution 1 mM of [Re(bpy)(CO)₃Cl] in 5% v/v H₂O/EMIM.

405 H₂ and CO were identified and quantified using a gas chromatograph (SRI 8610C) equipped
406 with a packed Molecular Sieve 5 Å column for permanent gases separation and a packed
407 Haysep-D column for light hydrocarbons separation. Argon (Linde 5.0) was used as carrier gas.
408 A flame ionization detector (FID) coupled to a methanizer was used to quantify CO while a
409 thermal conductivity detector (TCD) was used to quantify H₂. The liquid-phase products were
410 quantified using an ionic exchange chromatography system (883 Basic IC plus; Metrohm).

411

412

413 **Acknowledgements**

414 *The PhDs of D.G and S.P are financially supported from the European School on Artificial*
415 *Leaf: Electrodes & Devices (eSCALED) project. This work is part of the eSCALED project*
416 *which has received funding from the European's Union's Horizon 2020 research and*
417 *innovation programme under the Marie Skłodowska-Curie grant agreement No 765376.*

418 *This research used resources of the Electron Microscopy Service located at the University of*
419 *Namur. This Service is member of the "Plateforme Technologique Morphologie –Imagerie".*

420 *SEM images were also collected by F. Pillier at the Laboratoire Interfaces et Systèmes*
421 *Electrochimiques.*

422 *Parts of this work were supported by IPGP multidisciplinary program PARI, and by Paris–IdF*
423 *region SESAME Grant no. 12015908.*

424

425

427 **References**

- 428 [1] R. Francke, B. Schille, M. Roemelt, *Chem. Rev.* **2018**, *118*, 4631–4701.
- 429 [2] H. Takeda, C. Cometto, O. Ishitani, M. Robert, *ACS Catal.* **2017**, *7*, 70–88.
- 430 [3] N. Elgrishi, M. B. Chambers, X. Wang, M. Fontecave, *Chem. Soc. Rev.* **2017**, *46*, 761–
- 431 796.
- 432 [4] C. Sun, R. Gobetto, C. Nervi, *New J. Chem.* **2016**, *40*, 5656–5661.
- 433 [5] L. Sun, V. Reddu, A. C. Fisher, X. Wang, *Energy Environ. Sci.* **2020**, *13*, 374–403.
- 434 [6] T. R. O’Toole, L. D. Margerum, T. D. Westmoreland, W. J. Vining, R. W. Murray, T. J.
- 435 Meyer, *J. Chem. Soc., Chem. Commun.* **1985**, 1416–1417.
- 436 [7] C. R. Cabrera, H. D. Abruña, *J. Electroanal. Chem. Interfacial Electrochem.* **1986**, *209*,
- 437 101–107.
- 438 [8] J. Hawecker, J.-M. Lehn, R. Ziessel, *J. Chem. Soc., Chem. Commun.* **1983**, 536–538.
- 439 [9] A. Zhanaidarova, A. L. Ostericher, C. J. Miller, S. C. Jones, C. P. Kubiak,
- 440 *Organometallics* **2019**, *38*, 1204–1207.
- 441 [10] S. Cosnier, A. Deronzier, J.-C. Moutet, *J. Electroanal. Chem. Interfacial Electrochem.*
- 442 **1986**, *207*, 315–321.
- 443 [11] T. Yoshida, K. Tsutsumida, S. Teratani, K. Yasufuku, M. Kaneko, *J. Chem. Soc., Chem. Commun.* **1993**, 631–633.
- 444
- 445 [12] S. Oh, J. R. Gallagher, J. T. Miller, Y. Surendranath, *J. Am. Chem. Soc.* **2016**, *138*, 1820–
- 446 1823.
- 447 [13] J. Willkomm, E. Bertin, M. Atwa, J.-B. Lin, V. Birss, W. E. Piers, *ACS Appl. Energy*
- 448 *Mater.* **2019**, *2*, 2414–2418.
- 449 [14] J. D. Blakemore, A. Gupta, J. J. Warren, B. S. Brunshwig, H. B. Gray, *J. Am. Chem.*
- 450 *Soc.* **2013**, *135*, 18288–18291.
- 451 [15] A. Zhanaidarova, S. C. Jones, E. Despagnet-Ayoub, B. R. Pimentel, C. P. Kubiak, *J. Am.*
- 452 *Chem. Soc.* **2019**, *141*, 17270–17277.
- 453 [16] K. Shen, L. Zhang, X. Chen, L. Liu, D. Zhang, Y. Han, J. Chen, J. Long, R. Luque, Y.
- 454 Li, B. Chen, *Science* **2018**, *359*, 206–210.
- 455 [17] M. Wu, Y. Li, Z. Deng, B. L. Su, *ChemSusChem* **2011**, *4*, 1481–1488.
- 456 [18] S. Suter, S. Haussener, *Energy Environ. Sci.* **2019**, *12*, 1668–1678.
- 457 [19] J.-P. Song, L. Wu, W.-D. Dong, C.-F. Li, L.-H. Chen, X. Dai, C. Li, H. Chen, W. Zou,
- 458 W.-B. Yu, Z.-Y. Hu, J. Liu, H.-E. Wang, Y. Li, B.-L. Su, *Nanoscale* **2019**, *11*, 6970–
- 459 6981.
- 460 [20] M. L. Clark, P. L. Cheung, M. Lessio, E. A. Carter, C. P. Kubiak, *ACS Catal.* **2018**, *8*,
- 461 2021–2029.
- 462 [21] B. A. Rosen, A. Salehi-Khojin, M. R. Thorson, W. Zhu, D. T. Whipple, P. J. A. Kenis,
- 463 R. I. Masel, *Science* **2011**, *334*, 643–644.
- 464 [22] D. C. Grills, Y. Matsubara, Y. Kuwahara, S. R. Golisz, D. A. Kurtz, B. A. Mello, *J. Phys.*
- 465 *Chem. Lett.* **2014**, *5*, 2033–2038.
- 466 [23] J. Agarwal, R. P. Johnson, G. Li, *J. Phys. Chem. A* **2011**, *115*, 2877–2881.
- 467 [24] A. J. Morris, G. J. Meyer, E. Fujita, *Acc. Chem. Res.* **2009**, *42*, 1983–1994.
- 468 [25] X. Zheng, G. Shen, C. Wang, Y. Li, D. Dunphy, T. Hasan, C. J. Brinker, B. L. Su, *Nat.*

- 469 *Commun.* **2017**, *8*, 1–9.
- 470 [26] J. M. Smieja, C. P. Kubiak, *Inorg. Chem.* **2010**, *49*, 9283–9289.
- 471 [27] B. Reuillard, K. H. Ly, T. E. Rosser, M. F. Kuehnel, I. Zebger, E. Reisner, *J. Am. Chem.*
- 472 *Soc.* **2017**, *139*, 14425–14435.
- 473